Stringent upper limit of CH_4 on Mars based on SOFIA/EXES observation

S. Aoki[1,2,3], M. J. Richter[4], C. DeWitt[4], A. Boogert[5], T. Encrenaz[6], H. Sagawa[7], H. Nakagawa[3], A. C. Vandaele[1], M. Giuranna[8], T. K. Greathouse[9], T. Fouchet[6], A. Geminale[8], G. Sindoni[8], M. McKelvey[5], M. Case[4], and Y. Kasaba[3]

[1] Planetary Aeronomy, Belgian Institute for Space Aeronomy, 3 av. Circulaire, B-1180 Brussels, Belgium

[2] Fonds National de la Recherche Scientifique, rue d'Egmont 5, B-1000 Brussels, Belgium

[3] Department of Geophysics, Tohoku University, Sendai, Miyagi 980-8578, Japan

[4] Physics Department, University of California, Davis, CA 95616, USA

[5] Universities Space Research Association, Stratospheric Observatory for Infrared Astronomy, NASA Ames Research Center, MS 232-11, Moffett Field, CA 94035, USA

[6] LESIA, Observatoire de Paris, PSL Research University, CNRS, Sorbonne Universités, UPMC Univ. Paris 06, Univ. Paris Diderot, Sorbonne Paris Cité, 5 place Jules Janssen, 92195 Meudon, France

[7] Faculty of Science, Kyoto Sangyo University, Motoyama, Kamigamo, Kita-ku, Kyoto 603-8555, Japan

[8] Istituto di Astrofisica e Planetologia Spaziali, Istituto Nazionale di Astrofisica, Via del Fosso del Cavaliere 100, 00133 Roma, Italy

[9] Southwest Research Institute, Div. #15, San Antonio, TX 78228, USA

Abstract

Discovery of CH_4 in the Martian atmosphere has led to much discussion since it could be a signature of biological/geological activities on Mars. However, the presence of CH_4 and its temporal and spatial variations are still under discussion because of the large uncertainties embedded in the previous observations. We performed sensitive measurements of Martian CH_4 by using the Echelon-Cross-Echelle Spectrograph (EXES) onboard the Stratospheric Observatory for Infrared Astronomy (SOFIA) on 16 March 2016, which corresponds to summer (Ls = 123.2°) in the northern hemisphere on Mars. The high altitude of SOFIA (~13.7 km) enables us to significantly reduce the effects of terrestrial atmosphere. Thanks to this, SOFIA/EXES improves the chance to detect Martian CH_4 lines because it reduces the impact of telluric CH_4 on Martian CH_4, and allows us to use CH_4 lines in the 7.5 μm band which has less contamination. However, our results show no unambiguous detection of Martian CH_4. The Martian disk was spatially resolved into 3 x 3 areas, and the upper limits on the CH_4 volume mixing ratio range from 1 to 6 ppb. These results emphasize that release of CH_4 on Mars is sporadic and/or localized if the process is present.

1. Introduction

The presence of CH_4 in the Martian atmosphere has led to much discussion since it could be a signature of on-going and/or past biological/geological activities on Mars (e.g., Atreya et al., 2007). In 2004, the first detection of CH_4 on Mars was reported from the observations by the Planetary Fourier Spectrometer (PFS) onboard the Mars Express (MEx) spacecraft (Formisano et al., 2004). The mean abundance of CH_4 was found to be ~ 10 ppb. In the same year, detection of CH_4 was also reported by ground-based observations with the Canada-France-Hawaii Telescope (CFHT) / Fourier Transform Spectrometer (FTS) (Krasnoplsky et al., 2004). Theses discoveries of CH_4 on Mars were remarkable because its source could be either biological activity (e.g., subsurface micro-organisms) and/or hydrothermal activity (e.g., serpentinization) (Atreya et al., 2007). Identification of the source of CH_4 is very valuable for advancing not only planetary science but also future life explorations on Mars.

After 2004, Martian CH_4 has been investigated with remote-sensing observations by four groups, two from spacecraft-borne observations (Geminale et al., 2008; Geminale et al., 2011; Fonti and Marzo, 2010), and two from ground-based observations (Mumma et al., 2009; Krasnopolsky, 2012; Villanueva et al., 2013). The spacecraft-born PFS measurements showed the variations of CH_4 amounts depending on season, location, and localtime on Mars (Geminale et al., 2008: Geminale et al., 2011). In particular, an enhancement of CH_4 (~60 ppb) over the north polar cap during the northern summer was reported, which implied the possible presence of a CH_4 reservoir associated with the polar cap (Geminale et al., 2011). In contrast, Fonti and Marzo (2010) analyzed the data obtained with another spacecraft-born instrument (Thermal Emission Spectrometer (TES) onboard Mars Global Surveyor (MGS)) and found substantially different spatial and seasonal distributions, with peak abundance near 70 ppb over low-latitudes (Tharsis, Arabia Terra, and Elysium). Meanwhile, the other two groups investigated CH_4 on Mars using high-resolution, infrared spectrographs on ground-based facilities. Mumma et al. (2009) found extended plumes of CH_4 (~ 40 ppb) during the northern summer over low-latitude regions (Terra Sabae, Nill Fossae, and Syrtis Major) from IRTF/CSHELL observations performed in 2003. However, the same group reported no detection of CH_4 during their follow-up observations in 2006, 2009, and 2010 (Villanueva et al., 2013). They derived an upper limit of 7 ppb from those non-detection observations, which is generally smaller than the seasonal variations reported by the spacecraft-borne measurements groups. By contrast, Krasnopolsky (2012) claimed the detection of CH_4 (0-20 ppb) over Valles Marines using ground-based IRTF/CSHELL observations performed in late January 2006, just 28 days after Villanueva et al. (2013) observations, where no CH_4 had been observed over the same region (upper limit 7.8 ppb).

In short, these remote-sensing observations suggest a significant variability of CH_4 in space and time. From these observations, the lifetime of CH_4 in the Martian atmosphere is estimated to be on order of days to weeks. In contrast, the standard photochemical models showed that the lifetime of CH_4 in the Martian atmosphere is about 300-600 years (Lefevre and Forget, 2009), and, as a consequence, CH_4 should be uniformly distributed in the atmosphere. This discrepancy between the observed variability and the model prediction has led to much debate on the reliability of the previous remote-sensing observations. The reason behind such a debate is that the detected signal of CH_4 is very weak and the observations had a large uncertainty because of contamination of terrestrial lines and the need for a high signal-to-noise ratio. The previous ground-based observations used lines in the P-branch or R-branch of 3.3 μm band. The widths of these lines (half width at half maximum (HWHM)) are about 0.006 cm^{-1}, which is 5-10 times narrower than the spectral resolutions of CSHELL, NIRSPEC and CRIRES. In addition, the terrestrial atmosphere hampers the observation due to telluric CH_4 and its isotopes; their contribution to the observed spectrum must be separated from the Martian CH_4 contribution to the spectrum. Zahnle et al. (2010) pointed out that contamination from telluric $^{13}CH_4$ lines would be fatal in this aspect, being 10-50 times stronger than the Martian CH_4 lines (see **Fig. 1**). On the other hand, spacecraft-born observations (i.e., MGS/TES and MEx/PFS) are free from such contamination of the terrestrial atmosphere. However, their spectral resolutions are not enough for an unambiguous identification of CH_4. Even at the highest spectral resolution of PFS (~1.3 cm^{-1}) and even the fact that PFS observes the strongest lines of the Q-branch of 3.3 μm band, the absorption depth of 10 ppb of CH_4 yields only about 1 percent of the continuum emission, which is difficult to be distinguished from side lobes caused by strong solar lines. The spectral resolution of the TES instrument is ~5 times worse than that of PFS. Indeed, Fonti et al. (2015) carefully revisited their previous results from the MGS/TES measurements, and concluded that they are either not able to be confirmed or refuted.

Very recently, in-situ observations of CH_4 on Mars were performed by the Tunable Laser Spectrometer (TLS) onboard Curiosity rover (Webster et al., 2013; Webster et al., 2015). TLS detected CH_4 signal and showed strong variability of the amount (0-9 ppb). However, since TLS can measure CH_4 variation only on the Gale crater (which is the landing site of the rover), sensitive remote-sensing observation is still important to search for the source. Moreover, note that because there is residual terrestrial CH_4 gas in the foreoptics chamber of the TLS instrument (Webster et al., 2015), there is a debate on the reliability of this detection. Thus, it is still indispensable to confirm the presence of CH_4 on Mars.

The Echelon-Cross-Echelle Spectrograph (EXES) onboard the Stratospheric Observatory for

Infrared Astronomy (SOFIA) has unique capabilities to perform a sensitive search for CH_4 from Earth. Through the entire spectral range, the strongest CH_4 lines are located at 3.3 μm and 7.5 μm. **Fig. 1** shows the terrestrial and Martian spectra around the CH_4 lines at 3038.498 cm^{-1} (3.291 μm) and 1327.0742 cm^{-1} (7.535 μm), that are simulated for the IRTF/CSHELL and SOFIA/EXES observations, respectively (note that the terrestrial transmittances shown in **Fig. 1** are calculated for the best and worst airmass conditions of Mauna Kea and SOFIA observations, respectively). As shown in **Fig. 1**, one of the advantages of the 7.5 μm band is less contamination of minor terrestrial lines such as $^{13}CH_4$ or O_3 even though the intrinsic intensities of the CH_4 lines at 3.3 μm and 7.5 μm are comparable. However, observations of Martian CH_4 using this band are impossible from ground-based observatories because of terrestrial CH_4. Encrenaz et al. (2005) attempted to search for CH_4 on Mars using IRTF/TEXES in the mid-infrared spectral range, however, they could not use the strongest lines because of the deep terrestrial CH_4 absorption. This imposed a limitation on their data (derived upper limits were 20 ppb in the morning side and 70 ppb in the evening side). The situation changes drastically for SOFIA thanks to the higher altitude (~13.7 km). With SOFIA, Martian CH_4 lines at the 7.5 μm band can be measured in the wing of the terrestrial lines, which makes this air-borne facility quite unique compared to any other ground-based facilities including those located at the summit (~4 km in the altitude) of Mauna Kea. In order to detect the narrow Martian CH_4 lines located at the wings of the deep terrestrial line, high spectral resolution is essential. The EXES instrument realizes high spectral resolution of ~90,000, and it largely improves the chances to detect CH_4 lines although the Martian lines are not fully resolved. SOFIA/EXES can provide a few or several times better signals of Martian CH_4 than those by previous ground-based observations with less contamination of the minor telluric lines. Moreover, EXES has an additional advantage that we can measure multiple CH_4 lines simultaneously, which allows us to improve the accuracy of the CH_4 retrieval.

In this study, we describe the results of our sensitive search of CH_4 on Mars using SOFIA/EXES. The details of the SOFIA/EXES observations and data analysis are described in Section 2 and 3, respectively. The observational results are discussed in Section 4.

2. Observations

SOFIA is an airborne observatory consisting of a specially modified Boeing 747SP with a 2.7 m diameter telescope flying at altitudes as high as 13.7 km (Young et al., 2012). EXES is an infrared grating spectrograph onboard the SOFIA telescope. It is derived from the Texas Echelon Cross Echelle Spectrograph (TEXES) instrument in operation at NASA IRTF and Gemini-North (Lacy et al. 2002). EXES operates in the spectral ranges between 4.5 and 28.3 μm (350−2220 cm^{-1}),

with high spectral resolution mode (R=50,000−100,000), medium resolution mode (R=5,000−20,000), and low resolution mode (R=1,000−3,000). The instrument is equipped with a 1024 × 1024 Si:As detector array. The high-resolution mode is provided by a steeply blazed aluminum reflection grating used as an echelon, associated with an echelle grating to cross-disperse the spectrum (Richter et al. 2010).

Our observations using SOFIA/EXES were performed on 16 March 2016 (see Table 1). The observations were performed when SOFIA was flying at 13.7 km. The observed season on Mars corresponds to summer (*Ls* = 123.2°) in the northern hemisphere. The diameter of Mars was about 10 arcsec. The Doppler shift between Mars and Earth was -16.2 km/s. During the observation, the longitude of the sub-earth and sub-solar points varied from 247°W to 253°W, and from 213°W to 220°W, respectively. The latitude of these points was 7.7 °N (sub-earth) and 21.1°N (sub-solar). For our search of CH_4 on Mars, we selected the 1326-1338 cm^{-1} (7.47 - 7.54 μm) interval considering the availability of multiple strong CH_4 lines, and used the high-spectral resolution mode to improve the possibility of detecting the narrow Martian lines. The narrowest slit-width (1.44 arcsec) was used to maximize the spectral resolving power that provided an instrumental resolving power of ~90,000. The slit length is 10.69" (0.18 arcsec/pix), which is comparable to the diameter of Mars (~10"). **Fig. 2** illustrates the configuration of the slit positions. The slit was oriented at a position angle of 260°. As shown in **Fig. 2**, we observed the planet at three separate slit positions: which we called center, right, and left of the Martian disk. For the right and left positions, the center of the slit was offset by 2.5" perpendicular to the slit angle. At each slit position, we observed Mars for several minutes to reach the signal to noise ratio of more than ~200 with respect to the continuum emission. We nodded the telescope observing Mars and sky in A and B positions, respectively, with a motion of 20 arcsec perpendicular to the slit. Subtraction of (A–B) removes the telluric emissions and other background emission. In addition, we observed *alpha Lyr* as a telluric calibration star.

An example of the spectrum measured with EXES is shown in **Fig. 3**. We recorded 17 different spectral orders, covering 1326.57 - 1338.66 cm^{-1}. We selected this wavelength region based on the expected strengths of Martian CH_4 lines and the terrestrial atmosphere from SOFIA. The spectral coverage of EXES allows us to observe not only CH_4 but also H_2O, HDO, and CO_2 lines. The spatial resolution of SOFIA at the time of the observations was roughly 3 arcsec. This corresponds to a latitudinal/longitudinal resolution of about ±27° (~2000 km in the horizontal scale) at the sub-Earth point.

3. Data analysis

3.1. Extraction of the Martian features

We searched for CH_4 on Mars using multiple lines. As shown in **Fig. 3**, there are 11 strong CH_4 absorption lines in the selected spectral range. We confined our analysis to three lines that have no contamination from other lines (i.e., terrestrial CH_4 and H_2O, and Martian CO_2 and H_2O lines) and stronger intensities than the other CH_4 lines. **Table 2** describes the CH_4 lines used for this analysis. The line parameters were obtained from the HITRAN 2012 database (Rothman et al., 2013).

In order to increase the signal to noise ratio, the measured spectra were binned over 15 pixels (~2.7") along the slit which binning size is determined from the spatial resolution of the telescope. As a consequence, 3 averaged spectra were obtained for each slit position (see **Fig. 2**). The Martian CH_4 lines should appear on the wings of the deep terrestrial lines. **Fig. 4a** shows an example of an averaged EXES spectra around the CH_4 line at 1327.074219 cm^{-1}. As shown in **Fig. 4a**, the terrestrial and Martian CH_4 lines were clearly separated. Then, the absorption feature of Martian CH_4 lines were examined by fitting a local continuum level around the CH_4 lines. This local continuum was determined by fitting the averaged spectra with a cubic polynomial for the spectral interval of 25 points centered at the Martian CH_4 lines. The fitting did not include 17 center points where Martian CH_4 is expected. **Fig. 4b** shows an example of the local continuum determined by the cubic polynomial fit. The Martian CH_4 lines were extracted by obtaining the deviation of the observed spectrum from the local continuum, and then they were compared with synthetic spectra calculated by radiative transfer model.

3.2. Modeling of synthetic spectra

We performed radiative transfer calculations to evaluate (the upper limit on) CH_4 abundances in the extracted Martian features. We used a fast and accurate radiative transfer model that includes multiple scattering effects (Ignatiev et al., 2005). The calculation was performed in the spectral ranges between 1325 and 1340 cm^{-1}. Dust, water ice clouds, CO_2 gas, and CH_4 gas absorption were taken into account in the calculation. The vertical domain in the modeled Mars atmosphere was represented by 80 layers which covers altitudes from the surface to 80 km with uniform thickness of 1 km. The absorption coefficients of CO_2 and CH_4 gases were calculated based on the line-by-line method with a spectral sampling of 0.00025 cm^{-1} (about 1/60 of the spectral resolution of the measurements) using the HITRAN 2012 database (Rothman et al., 2013). For the line shape function, a Voight function was adopted (Kuntz, 1997; Ruyten, 2004). The single scattering optical properties of dust and water ice clouds were calculated with the Mie-theory (Wiscombe, 1980) and then integrated with the modified gamma distribution (Kleinbohl et al., 2009). The refractive

indices of dust and water ice were from the works by Wolf and Clancy (2003) and Warren (1984), respectively.

Geometry and orbital parameters during the observations such as emission angles, latitude, and longitude of Mars were obtained from the NASA-JPL ephemeris generator (http://ssd.jpl.nasa.gov/horizons.cgi). Based on that, we computed the synthetic spectra over the Martian disk with an interval of 0.25 arcsec. Surface temperatures and vertical profiles of temperature, pressure, dust, water ice clouds, and CO_2 volume mixing ratio were extracted from the Mars Climate database (MCD) ver 5.2 for the each spatial point over the Martian disk (Millour et al., 2015). In order to take into account the spatial resolution of the observations, the calculated synthetic spectra were synthesized with a two-dimentional Gaussian function with a full width at half maximum (FWHM) of 3 arcsec. The synthesized spectra were averaged over the expected slit position to be compared with the measured spectra. The averaged synthetic spectra were finally convolved in a wavelength domain with another Gaussian function that corresponds to the spectral resolution of EXES (R=90,000; ~9 pixels).

3.3. Validation of the data reduction methodology

To check the validity of the extraction method and calculation of synthetic spectra, the algorithm was applied to Martian CO_2 lines as well. For this purpose, a weak CO_2 isotope (638) line at 1326.75438 cm^{-1} and CO_2 isotope (628) line at 1327.917522 cm^{-1} were selected. The line intensity of the CO_2 (638) line is 9.662 x 10^{-27} cm at 296 K with an uncertainty range between 2 % and 5 %, and that of the CO_2 (628) line is 1.883 x 10^{-26} cm with an uncertainty range being more than 20 % (Rothman et al., 2013). **Fig. 5** shows examples of the extraction of these CO_2 lines by using the local continuum determined by the cubic polynomial fit, and their comparison with the synthetic spectra calculated by our radiative transfer model. The Martian CO_2 (638) line yields about 10 % of absorption depth respect to the continuum emission, while the CO_2 (628) line does a few percent of absorption because the Lower-state energy *E"* of the CO_2 (628) line (*E"* = 1052.7719 cm^{-1}) is larger than that of CO_2 (638) line (*E"* = 170.0769 cm^{-1}). The extracted spectral features of the Martian CO_2 lines show a good agreement with the synthetic spectra (note that the volume mixing ratio of CO_2 considered in the synthetic spectra is the one extracted from MCD, and the isotopic ratio of CO_2 is the terrestrial one included in HITRAN 2013).

3.4. Retrieval of CH_4 mixing ratio

The synthetic spectra were calculated for CH_4 volume mixing ratios ranging from 0 ppb to 50 ppb with intervals of 1 ppb, and the best-fit CH_4 mixing ratio was determined by minimizing the

cost function C. The cost function was defined as

$$C = \sum (Y_{obs} - Y_{model})^2 ,$$

where $Y_{model}(x)$ is transmittance of synthetic spectra which is the synthetic spectra with CH_4 divided by the one without CH_4, and Y_{obs} is transmittance of the EXES spectra which is the original SOFIA spectra divided by continuum simulated via Cubic polynomial fitting (as described in 3.1). The cost functions were calculated using the spectral interval of 25 points centered at the Martian CH_4 lines. The retrievals were performed independently for each line of the selected three CH_4 lines. **Fig. 4c** shows an example of the comparison between the transmittance of the EXES spectra and synthetic ones.

The uncertainty in the retrieved CH_4 mixing ratio were carefully estimated via statistics using simulated EXES spectra and the following steps:

- Simulated EXES spectra in the relevant spectral region were calculated using the spectral resolution and sampling of the actual measurements considering the US standard earth atmosphere above 14 km with the airmass set to match the actual observation condition. Mars atmospheric absorption due to CO_2 gas is also included in this simulated spectra. Instrumental noise was input to the simulated EXES spectra. The instrumental noise were defined by

$$Noise = \sqrt{\frac{C}{N}} \times \xi ,$$

  where N is the number of spectral points (i.e., 25) and ξ is a random number following a Gaussian distribution (σ=1). The first value in the equation represents the standard deviation between the best-fit model and the measured EXES spectra. To initialize the random number, a total of 100 different "seed" values were used (i.e., we have different 100 noise patterns in total).
- Martian CH_4 absorptions were additionally included to the simulated EXES spectra. CH_4 volume mixing ratios from 0 to 30 ppb with intervals of 1 ppb were considered (i.e., 3100 simulated EXES spectra were obtained in the end).
- The CH_4 retrieval algorithm, which we used for the data analysis of the real measurement data, was applied to these simulated EXES spectra in a similar way. Such retrieval tests provide an estimate on the accuracy of the retrieved CH_4 mixing ratios. **Fig. 4d** shows an example of our retrieval test.

After the uncertainties were evaluated for the results of each CH_4 line, the CH_4 mixing ratios and their 3σ confidences were calculated by the weighted averages using the ones retrieved from three CH_4 lines independently (see Section 3 of Aoki et al., 2015).

4. Results and Discussions

Table 3 summarizes the CH_4 volume mixing ratios independently retrieved from the selected CH_4 lines, their weighted averages, and the corresponding locations (latitude and longitude) and local times. The results from three lines were all consistent within 3σ. As shown in **Table 3**, there are no definitive detections of CH_4. The upper limits range from 1 to 6 ppb, which are more stringent than those by the previous remote-sensing observations.

The SOFIA/EXES observation covers Nili Fossae and Syrtis Major (10°S-30°N, 300-330°W) where Mumma et al. (2009) had reported the presence of extended plumes of CH_4 (~ 40 ppb). The observing season of this study is almost the same with those Mumma et al. (2009) although the Martian Year is different (their IRTF/CSHELL observation was performed at *Ls*=122° in MY 26; the SOFIA/EXES observation at *Ls*=123° in MY 33). As roughly half of the field of view of an averaged SOFIA/EXES spectrum corresponds to the signal from Nili Fossae and Syrtis Major, our measurement are capable of detecting such a CH_4 plume if it exists. However, the results show that the CH_4 mixing ratio of 2 ± 4 ppb for the location covering Nili Fossae and Syrtis Major. Non-detection of such a plume by SOFIA/EXES indicates that the release of CH_4 is very unlikely an annual event.

Fries et al. (2016) recently proposed a candidate of the CH_4 enhancement. The hypothesis is that carbonaceous material is deposited into the Martian atmosphere in meteor showers and then ambient UV generates CH_4 from that. Indeed, the CH_4 plume reported by Mumma et al. (2009) was measured only a couple of days after a Mars encounter with the orbit of comet C/2007 H_2 Skiff. However, Roos-Serote et al. (2016) argued that there is no correlation between high atmospheric CH_4 abundance and the occurence of meteor showers after considering a full set of CH_4 observations including new Curiosity/TLS observations and all the predicted meteor shower events. The comet Skiff encountered Mars again on 8 March 2016, which is just 8 days before we performed our observations with SOFIA/EXES. The non-detections of such CH_4 plumes by SOFIA/EXES support the argument that the meteor shower does not likely produce high CH_4 abundances in the Mars atmosphere.

The SOFIA/EXES observation also covers Gale Crater (Latitude=4.5°S, Longitude=137°E) where Curiosity/TLS has been measuring CH_4 abundances. TLS revealed that background level of CH_4 mixing ratio over Gale Crater is 0.69 ± 0.25 ppb, and detected higher amount of CH_4 mixing ratio (5-9 ppb) at *Ls*=336.5° in MY 31 and *Ls*=55°-82° in MY 32 (Webster et al., 2015). However, in MY 33, TLS does not detect such high amounts of CH_4 till Ls=94.2° (Roos-serote et al., 2016). Our results show that the CH_4 mixing ratio covering Gale Crater is 1 ± 1 ppb, 0 ± 3 ppb, and 0 ± 1 ppb. The upper limits are larger than the TLS-reported background level but less than the high

value. The SOFIA/EXES observation was carried out at Ls=123.2° in MY 33, which is out of the seasonal range of high CH_4 abundance observed by TLS. One possible explanation for this non-detection of CH_4 by SOFIA/EXES could be due to strong temporal variation.

SOFIA/EXES is probably the most accurate remote-sensing facility for detecting CH_4 from Earth. However, our result did not show unambiguous detection of CH_4. Non-detection of CH_4 could be due to its strong temporal variation similar to what Curiosity/TLS has been measuring over Gale crater, or localized spatial distribution. Our results emphasize that release of CH_4 on Mars is sporadic and/or localized if the process is present.

Figures and Tables

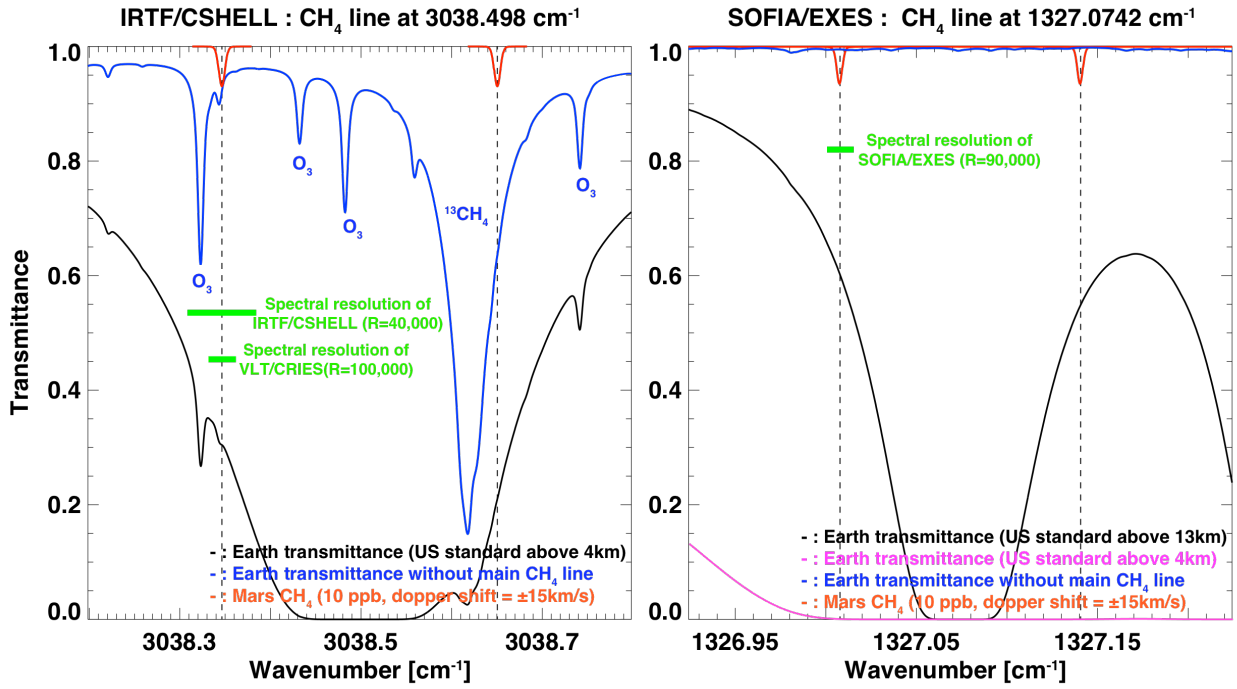

Figure 1: Synthetic spectra around the CH_4 line at 3038.498 cm^{-1} (left) and at 1327.0742 cm^{-1} (right). The former spectral region was used for the previous observations performed by IRTF/CSHELL, Keck/NIRSPEC, and VLT/CRIRES (e.g., Mumma et al., 2009; Villanueva et al., 2013), and the latter one was used for the SOFIA/EXES observations. The black and blue curves in the left figure represent the transmittance with/without the main CH_4 line due to terrestrial atmosphere calculated from US standard atmosphere above 4 km (which is the altitude of Mauna Kea Observatory) with airmass = 1.4 (which is the minimum airmass during the observation on 20 March 2003 by Mumma et al. (2009).). The black and blue curves in the right figure are the transmittances calculated from US standard atmosphere above 14 km (which is the altitude of SOFIA) with airmass = 2.0 (which is the maximum airmass during our observation on 16 March

2016). The purple curve shown in the right figure is the same as black one but from US standard atmosphere above 4 km. The red curves shown in both figures are transmittance due to 10 ppb of Martian CH_4 with the Doppler shift between Mars and Earth being ± 15 km/s. The green bars shown in the left and right figures represent the spectral resolutions of IRTF/CSHELL and VLT/CRIRES, and that of SOFIA/EXES, respectively.

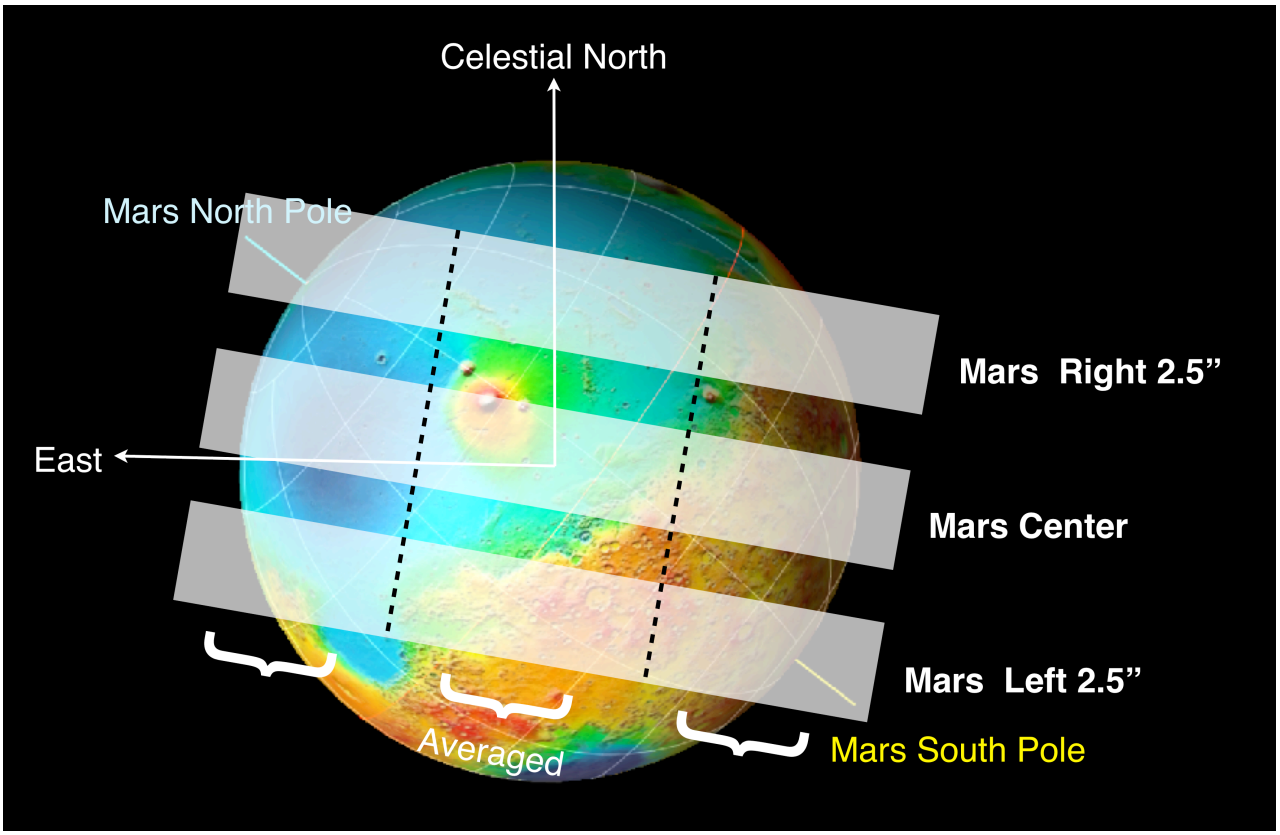

Figure 2: Geometry of the Mars observations taken by SOFIA/EXES. The instrument slit was oriented at a position angle of 260°. The slit is indicated as white boxes, and were put at the three separate slit positions: 'Mars Center', 'Mars Right 2.5', and 'Mars Left 2.5'. For the center position, the slit was placed over the sub-Earth point. For the right and left positions, we offset the center of the slit to 2.5" perpendicular to the slit angle. In this analysis, the measured spectra were binned over 15 pixels (~2.7") along the slit in order to increase the signal to noise ratio. As a consequence, 3 averaged spectra were obtained for each slit position.

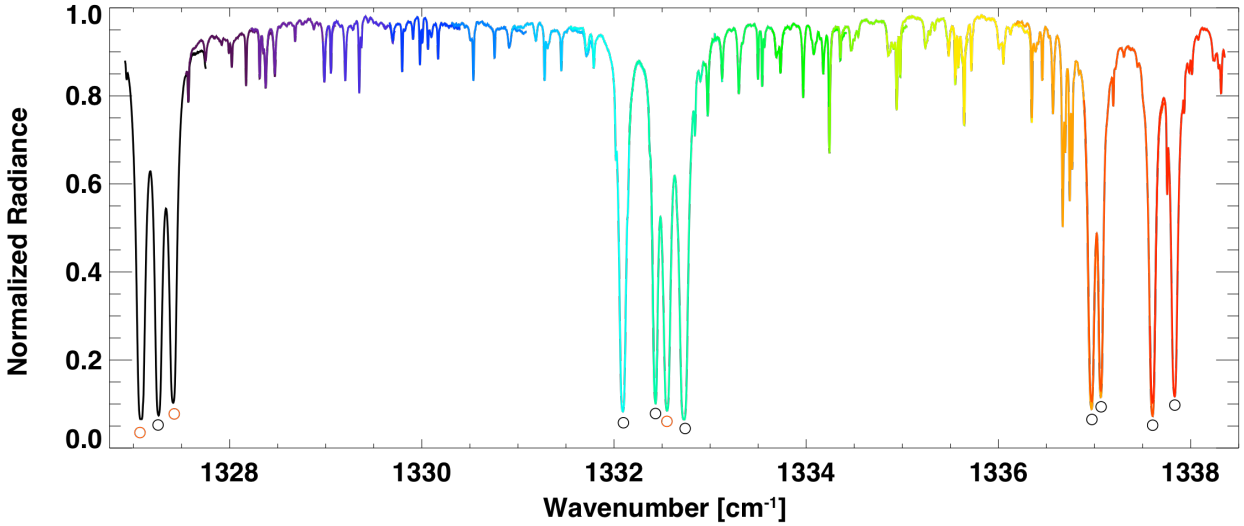

342

343 **Figure 3**: Example of a Mars spectrum obtained by SOFIA/EXES, spatially integrated over the slit.
344 Differences in colors show the 17 spectral orders. The spectrum was observed on 16 March 2016
345 with 9 minutes integration. Circular symbols represent the strong terrestrial CH_4 lines. The red
346 ones are the CH_4 lines that are used in this analysis. The other lines visible in this spectrum are
347 H_2O, HDO, CO_2 (628), and CO_2 (638).

348

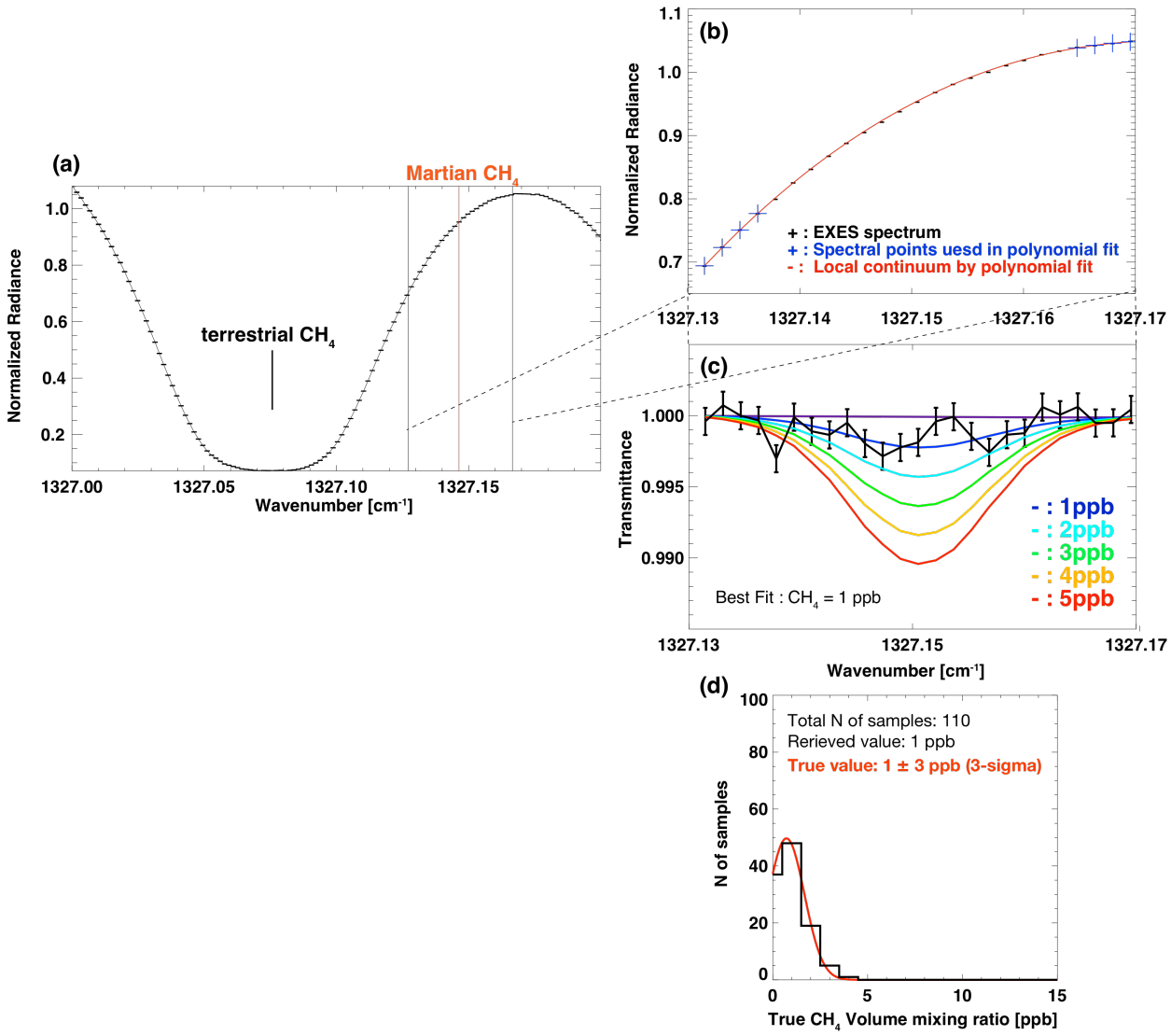

349

350 **Figure 4**: An example of data analysis. **(a)** The black curve shows the averaged EXES spectrum in
351 the spectral range between 1327.0 and 1327.2 cm^{-1}. The slit position is "Mars Center #1", and the
352 mean Latitude, Longitude, and Local time of the averaged spectrum are 40°N, 113°E, and 12h,
353 respectively. The strong absorption due the terrestrial CH_4 is visible at 1327.074219 cm^{-1}. The red
354 vertical bar shows the expected spectral position of the Martian CH_4 line shifted due to Doppler
355 velocity between Earth and Mars. The black bars represent the spectral range which was used for
356 retrieval of CH_4 mixing ratio on Mars. **(b)** The black points are the same EXES spectrum as shown
357 in (a) but focused around the expected Martian CH_4 lines. The red curve shows the local
358 continuum established by the cubic polynomial fit. The blue points represent the spectral points
359 used to perform the cubic polynomial fit. **(c)** The black curve shows the transmittance spectrum
360 due to Mars atmosphere that is the EXES spectrum divided by the local continuum. The color
361 curves are the synthetic transmittances with various mixing ratio of the Martian CH_4 (blue: 1 ppb,

light blue: 2 ppb, green: 3 ppb, orange: 4 ppb, red: 5 ppb) that is the synthetic spectrum with the Martian CH_4 divided by the one without the Martian CH_4. The one with 1 ppb of CH_4 mixing ratio (the blue one) provides the minimum cost function (i.e., the best-fit synthetic spectrum). **(d)** Histogram of true CH_4 mixing ratio when the retrieved CH_4 mixing ratio is 1 ppb. The histogram is obtained from the retrieval test using simulated EXES spectra (see Section 3.4). The uncertainty of this retrieval is estimated to be 3 ppb (3σ) from the histogram.

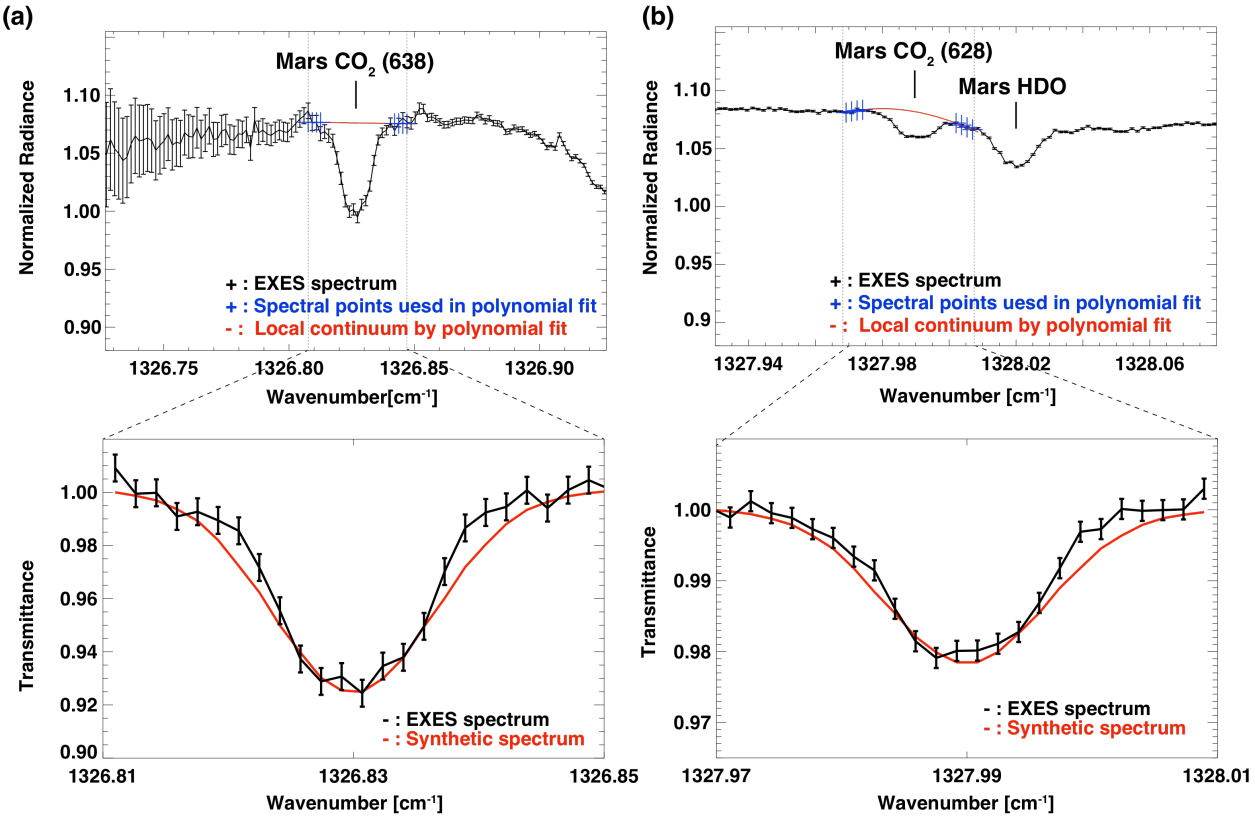

Figure 5: Examples of extraction of the Martian CO_2 lines and their comparison with the synthetic spectra calculated by our radiative transfer codes. Those of CO_2 (638) line at 1326.75438 cm^{-1} and CO_2 (628) line at 1327.917522 cm^{-1} are shown in Fig. (a) and (b), respectively. The positions of these lines are shifted due to the Doppler velocity between Mars and Earth. The black curves shown in the upper panels are the averaged EXES spectrum. The slit position is "Mars Center #1", and the mean Latitude, Longitude, and Local time of the averaged spectrum are 17°S, 179°E, and 16h, respectively. In the upper panel of fig. (b), an absorption band due Martian HDO is also visible. Note that error values in the left wing of the Martian CO_2 (638) line are relatively high because they are close to the edge of the slit. The red curves and blue points in the upper panels show the local continuums established by the cubic polynomial fit and the spectral points used to perform the cubic polynomial fit, respectively. In the lower panels, the black curves represent the

transmittance spectra due to Mars atmosphere that are the EXES spectrum divided by the local continuum. The red curves are the synthetic transmittances. The extracted spectral features of the Martian CO_2 lines show a good agreement with the synthetic spectra.

Table 1 Overview of the SOFIA/EXES observations.

Date and time (UT)	***Ls* (°)**	**MY**	**Doppler shift (km/s)**	**Diameter of Mars (″)**	**Aircraft Altitude (km)**	**Silt positions and integration times (min)**	**Sub Earth longitude (°W)**	**Spectral range (cm^{-1})**
16/March/2016 9:59–10:32	123.2	33	-16.2	10	13.7	Mars Center #1: 9 Mars Center #2: 6 Mars Left 2.5": 9 Mars Right 2.5": 9	247-253	1326.57 -1338.66

Table 2 Parameters of CH_4 lines used in this study. The values are taken from the HITRAN 2012 spectroscopic database (Rothman et al., 2013).

Wavenumber [cm^{-1}]	**Intensity [cm] (for 296 K)**	**Lower state Energy [cm^{-1}]**
1327.074219	9.631E-20	62.8781
1327.409783	5.781E-20	62.8757
1332.546743	5.732E-20	104.7746

Table 3 CH_4 mixing ratio on Mars retrieved from the SOFIA/EXES observation. Note that EXES spectra were spatially binned over ~2.7 arcsec, which corresponds latitudinal/longitudinal resolution of about ±27° at the sub-Earth point.

Slit position	Lat (°)	East Lon (°)	LT	CH_4 Volume mixing ratio (3σ)			
				1327.0742 cm^{-1}	1327.4098 cm^{-1}	1332.5467 cm^{-1}	**Weighted average**
Mars Center #1	-17	179	16	3 ± 5 ppb	1 ± 4 ppb	0 ± 14 ppb	**2 ± 3 ppb**
Mars Center #1	13	149	14	0 ± 2 ppb	1 ± 2 ppb	4 ± 6 ppb	**1 ± 1 ppb**
Mars Center #1	40	113	12	1 ± 3 ppb	1 ± 5 ppb	0 ± 7 ppb	**1 ± 2 ppb**
Mars Left	-42	155	15	0 ± 9 ppb	0 ± 6 ppb	0 ± 14 ppb	**0 ± 4 ppb**
Mars Left	-8	123	13	0 ± 7 ppb	0 ± 3 ppb	3 ± 12 ppb	**0 ± 3 ppb**
Mars Left	13	90	11	4 ± 6 ppb	0 ± 5 ppb	5 ± 14 ppb	**2 ± 4 ppb**
Mars Right	0	192	18	5 ± 6 ppb	0 ± 2 ppb	0 ± 2 ppb	**0 ± 2 ppb**
Mars Right	30	171	16	0 ± 2 ppb	2 ± 4 ppb	0 ± 9 ppb	**0 ± 2 ppb**
Mars Right	56	126	13	0 ± 2 ppb	0 ± 3 ppb	1 ± 3 ppb	**0 ± 1 ppb**
Mars Center #2	-17	172	16	2 ± 5 ppb	0 ± 5 ppb	0 ± 8 ppb	**1 ± 3 ppb**
Mars Center #2	13	143	14	0 ± 3 ppb	0 ± 2 ppb	3 ± 7 ppb	**0 ± 1 ppb**
Mars Center #2	40	107	12	0 ± 4 ppb	5 ± 8 ppb	0 ± 5 ppb	**1 ± 3 ppb**

Acknowledgements

This work has been supported by the FNRS "CRAMIC" project under grant agreement n° T.0171.16 and based on observations made with the NASA/DLR Stratospheric Observatory for Infrared Astronomy (SOFIA). SOFIA is jointly operated by the Universities Space Research Association, Inc. (USRA), under NASA contract NAS2-97001, and the Deutsches SOFIA Institut (DSI) under DLR contract 50 OK 0901 to the University of Stuttgart. MJR, CD, and MC of the EXES team are supported by NASA award NNX13AI85A. YK and NH are supported by a Grant-in-Aid for Scientific Research (15H05209; 16K05566) from the Japanese Society for the Promotion of Science (JSPS). HN was supported by the Astrobiology Center Program of National Institutes of Natural Sciences (NINS) (Grant Number AB281003).

438 **References**

439 Aoki, S., Nakagawa, H., Sagawa, H, Giuranna, M., Sindoni, G., Aronica, A., Kasaba, Y., 2015.
440 Seasonal variation of the HDO/H_2O ratio in the atmosphere of Mars at the middle of northern
441 spring and beginning of northern summer. Icarus 260, 7-22.

442 Atreya, S.K., Mahaffy, P.R., Wong, A., 2007. Methane and related trace species on Mars: Origin,
443 loss, implications for life, and habitability. Planet. Space Sci. 55, 358–369.

444 Encrenaz, T., Bézard, B., Owen, T., Lebonnois, S., Lefèvre, F., Greathouse, T., Richter, M., Lacy,
445 J., Atreya, S., Wong, A.S., Forget, F., 2005. Infrared imaging spectroscopy of Mars: H_2O
446 mapping and determination of CO_2 isotopic ratios. Icarus, 179, 43-54.

447 Fonti, S., Marzo, G.A., 2010. Mapping of methane on Mars. Astron. Astrophys. 512, A51.

448 Fonti, S., Mancarella, F., Liuzzi, G.. Roush, T.L.. Chizek Frouard, M., Murphy, Blanco, J., 2015.
449 Revisiting the identification of methane on Mars using TES data. Astron. Astrophys. 581,
450 A136.

451 Formisano, V., Atreya, S.K., Encrenaz, T., Ignatiev, N., Giuranna, M., 2004. Detection of methane
452 in the atmosphere of Mars. Science 306, 1758–1761.

453 Fries, M., Christou, A., Archer, D., Conrad, P., Cooke, W., Eigenbrode, J., Kate, I.L. ten, Matney,
454 M., Niles, P., Sykes, M., Steele, A., Treiman, A., 2016. A cometary origin for Martian
455 atmospheric methane, Geochem. Perspect. Lett., 2, 10–23.

456 Geminale, A., Formisano, V., Giuranna, M., 2008. Methane in Martian atmosphere: Average
457 spatial, diurnal, and seasonal behavior. Planet. Space Sci., 56(9), 1194–1203.

458 Geminale, A., Formisano, V., Sindoni, G., 2011. Mapping methane in Martian atmosphere with
459 PFS-MEX data. Planet. Space Sci. 59, 137–148.

460 Ignatiev, N.I., Grassi, D., Zasova, L.V., 2005. Planetary Fourier spectrometer data analysis: fast
461 radiative transfer models. Planet. Space Sci. 53, 1035–1042.

462 Kleinböhl, A., Schofield, J.T., Kass, D.M.. Abdou, W.A.. Backus, C.R.. Sen, B.; Shirley, J.H.,
463 Lawson, W.G., Richardson, M.I., Taylor, F.W., Teanby, N.A., McCleese, D.J, 2009. Mars
464 Climate Sounder limb profile retrieval of atmospheric temperature, pressure, and dust and water
465 ice opacity. , J. Geophys. Res., 114(E10), E10006.

466 Krasnopolsky, V.A, Maillard, J.P, Owen, T.C., 2004. Detection of methane in the Martian
467 atmosphere: evidence for life? Icarus 172, 53747.

468 Krasnopolsky, V.A., 2012. Search for methane and upper limits to ethane and SO_2 on Mars. Icarus,
469 217, 144–152.

470 Kuntz, M., 1997. A new implementation of the Humlicek algorithmfor the calculation of the Voigt
471 profile function. J. Quant. Spectrosc. Radiat. Transfer 57 (6), 819–824.

Lacy, J.H., Richter, M.J., Greathouse, T.K., Jaffe, D.T., Zhu, Q, 2002. TEXES: a sensitive high-resolution grating spectrograph for the mid-infrared. The publication of the Astronomical Society of the Pacific, 114, 792, 153-168.

Lefèvre, F., Forget, F., 2009. Observed variations of methane on Mars unexplained by known atmospheric chemistry and physics. Nature 460 (7256), 720–723.

Millour, E. et al., 2015. The Mars Climate Database (MCD version 5.2). European Planetary Science Congress 2015, id.EPSC2015-438.

Mumma, M.J., Villanueva, G.L., Novak, R.E., Hewagama, T., Bonev, B.P., DiSanti, M.A., Mandell, A.M., Smith, M.D., 2009. Strong release of methane on Mars in northern summer 2003. Science 323 (5917), 1041–1045.

Richter, M.J., Ennico, K.A., Mc Kelvey, M.E., Seifhart, A., 2010. Status of Echelon-cross-Echelle Spectrograph for SOFIA. Proc. SPIE7735 "Ground-based and Airborne Instrumentation for Astronomy - III", I.S. McLean, S. Ramsay and H. Takami edts., San Diego, Ca, USA.

Roos-Serote, M., Atreya, S.K., Webster, C.R., Mahaffy, P.R, 2016. Cometary origin of atmospheric methane variations on Mars unlikely. J. Geophys. Res., Planets, 121, doi:10.1002/2016JE005076.

Rothman, L.S., Gordon, I.E., Babikov, Y., Barbe, A., Chris Benner, D., Bernath, P.F., Birk, Bizzocchi, L., Boudon, V., Brown, L.R, Campargue, A., Chance, K., Cohen, E.A., Coudert, L.H., Devi, V.M., Drouin, B.J., Fayt, A., Flaud, J.-M., Gamache, R.R., Harrison, J.J., Hartmann, J.-M., Hill, C., Hodges, J.T., Jacquemart, D., Jolly, A., Lamouroux, J., Le Roy, R.J., Li, G., Long, D.A., Lyulin, O.M., Mackie, C.J., Massie, S.T., Mikhailenko, S., 2013. The HITRAN2012 molecular spectroscopic database. J. Quant. Spectrosc. Radiat. Transfer 130, 4-50.

Ruyten, W., 2004. Comment on ''A new implementation of the Humlicek algorithm for the calculation of the Voigt profile function'' by M. Kuntz [JQSRT 57(6) (1997) 819–824]. J. Quant. Spectrosc. Radiat. Transfer 86, 231–233.

Villanueva, G. L., Mumma, M.J. , Novak, R.E., Radeva, Y.L., Käufl, H.U., Smette, A., Tokunaga, A., Khayat, A., Encrenaz, T., Hartogh, P, 2013. A sensitive search for organics (CH_4, CH_3OH, H_2CO, C_2H_6, C_2H_2, C_2H_4), hydroperoxyl (HO_2), nitrogen compounds (N_2O, NH_3, HCN) and chlorine species (HCl, CH_3Cl) on Mars using ground-based high-resolution infrared spectroscopy, Icarus, 223, 11–27.

Warren, S..G., 1984. Optical constants of ice from ultraviolet to the microwave. Applied Optics, 23, 8, 1206-1225.

Wolff, M. J., and Clancy, R.T., 2003. Constraints on the size of Martian aerosols from thermal

emission spectrometer observations, J. Geophys. Res., 108(E9), 5097.

Webster, C.R., et al, 2013. Lower upper limit to methane abundance on Mars, Science, 342, 355–357.

Webster, C.R., et al, 2015. Mars methane detection and variability at Gale crater, Science, 347, 415–417.

Wiscombe, W.J., 1980. Improved Mie scattering algorithms. Applied Optics, 19, 9, 1505–1509.

Young, E.T., et al., 2012. Early Science with SOFIA, The Stratospheric Observatory for Infrared Astronomy. The Astrophysical Journal Letters, 749, L17.

Zahnle, K., Freedman, F.S., Catling, D.C., 2010. Is there Methane on Mars?, Icarus, 212, 493–503.